

Constraints on the Dark Side of the Universe and Observational Hubble Parameter Data

Tong-Jie Zhang^{1, 2, *} and Cong Ma^{1, †}

¹*Department of Astronomy, Beijing Normal University, Beijing 100875, P. R. China*

²*Center for High Energy Physics, Peking University, Beijing 100871, P. R. China*

This paper is a review on the observational Hubble parameter data that have gained increasing attention in recent years for their illuminating power on the dark side of the universe — the dark matter, dark energy, and the dark age. Currently, there are two major methods of independent observational $H(z)$ measurement, which we summarize as the “differential age method” and the “radial BAO size method”. Starting with basic cosmological notions such as the spacetime coordinates in an expanding universe, we present the basic principles behind the two methods. We further review the two methods in greater detail, including the source of errors. We show how the observational $H(z)$ data presents itself as a useful tool in the study of cosmological models and parameter constraint, and we also discuss several issues associated with their applications. Finally, we point the reader to a future prospect of upcoming observation programs that will lead to some major improvements in the quality of $H(z)$ data.

PACS numbers: 98.80.Es, 95.36.+x, 95.35.+d, 98.62.Ai, 98.62.Py, 98.65.Dx

* tjzhang@bnu.edu.cn

† cma@mail.bnu.edu.cn

I. INTRODUCTION

The expansion of our universe has been one of the greatest attractions of scientific talents since the seminal work of Edwin Powell Hubble [1] in 1929. Hubble’s compilation of observational distance-redshift (expressed in terms of radial velocity) data suggested a linear pattern of “extra-Galactic nebulae” (an archaic term for galaxies) receding from each other:

$$\dot{\mathbf{x}} = H\mathbf{x}, \quad (1)$$

where H is the proportional constant now bearing his name, and \mathbf{x} is the positional coordinates of a galaxy measured with our Galaxy as the origin.

The discovery of Hubble’s Law marked the commencement of the era of quantitative cosmology in which theories of the universe can be subjected to observational test. Since the days of Hubble, advances in technology have enabled astronomers to measure the light from increasingly deeper space and more ancient time, and our ideas of the entire history of the expanding universe have been gradually converging into a unified picture of Big Bang–Cold Dark Matter universe. In this picture, the dominating form of energy density transited from radiation to dark matter, and relics of primordial perturbation were imprinted on today’s observable CMB anisotropy and large-scale structures (LSS). This picture is obtained from its two ends: the CMB last-scattering surface at $z \approx 1000$ and the LSS around us at $z \approx 0$. The vast spacetime extent between both ends, in particular the era before reionization, remains mostly hidden from our view. In addition, the past two decades’ cosmological observations, especially those of type Ia supernovae (SNIa), indicated that the recent history of universal expansion is an acceleration, possibly driven by an unknown “dark energy” [2, 3] whose physical nature has not been identified.

Therefore it appears to us that our understanding of the universe is currently under the shade of three dark clouds — the mysterious *dark energy* that drives late-time accelerated expansion, the nature of *dark matter* that is vital to the formation of structures, and the unfathomable *dark age* that has not yet revealed itself to observations. This is the “3-D universe” in which possible answers to some of the most profound questions of physics are hidden.

In the face of these vast unknown sectors of the universe, any observational probe into its past history is invaluable. Recently, the direct measurement of the expansion rate, expressed in terms of the Hubble parameter $H(z)$, is gaining increasing attention. As a cosmological test, it can help with the determination of important parameters that affects the evolution of the universe, and reconstruct the history around key events such as the turning point from deceleration to acceleration. As an observable, it manifests itself in various forms in different eras, especially in the baryon acoustic oscillation (BAO) features in the LSS that may be detectable in the dark age.

This paper is a review on the current status of observational Hubble parameter data and its application in cosmology. In Section II we briefly review the cosmological background of an expanding universe. In Section III we present two important observational methods of $H(z)$ observation, their principles and implementations. Next, we review the important role of the observational $H(z)$ data in the study of cosmological models in Section IV. We will also discuss some issues associated with their application. Finally, in Section V, we briefly discuss some ongoing efforts that promise possible improvements over the current status of $H(z)$ measurements.

II. BACKGROUND

In this section, we will review some basic ideas and definitions in cosmology that must be kept in mind in order to understand and interpret the observational $H(z)$ data and their implications.

A. Spacetime, Metric, and Coordinates

The spacetime structure of the homogeneous, isotropic universe is characterized by the Friedmann-Robertson-Walker (FRW) metric

$$g_{\mu\nu} = \begin{pmatrix} -1 & & & \\ & a^2(t) & & \\ & & a^2(t) & \\ & & & a^2(t) \end{pmatrix}. \quad (2)$$

The presence of the scale factor $a(t)$ means that the spacetime is not necessarily static. In reality, we know that the universe is expanding, and $a(t)$ increases with time.

Using the metric (2), the infinitesimal spacetime interval scalar $ds^2 = dx_\nu dx^\nu = g_{\mu\nu} dx^\mu dx^\nu$ is obviously

$$ds^2 = -c^2 dt^2 + a^2(t) dx^i dx^i. \quad (3)$$

Here we have used the four-coordinate vector $x^\alpha = (ct, \mathbf{x}^i)$ that has the dimension of length.

It is often useful to express the spatial components of the four-coordinate vector, i.e. the “comoving position”, in dimensionless spherical coordinates $\mathbf{x}^i = (r, \theta, \phi)$ and give the scale factor the dimension of length. Under this convention, the spacetime interval (3) can be re-written as

$$ds^2 = -c^2 dt^2 + a^2(t) \left(\frac{dr^2}{1 - kr^2} + r^2 d\theta^2 + r^2 \sin^2 \theta d\phi^2 \right) \quad (4)$$

where k is one of $\{-1, 0, 1\}$. The parameter k is the sign of the Gaussian curvature of the space, and $k = 0$ if the universe is spatially flat.

We can further transform equation (4) by introducing the coordinate

$$\chi = \int_0^r \frac{dr'}{\sqrt{1 - kr'^2}} = \text{sinn}^{-1} r \quad (5)$$

where the sinn function is a shorthand notation:

$$\text{sinn } x = \begin{cases} \sin x & \text{for } k = 1, \\ x & \text{for } k = 0, \\ \sinh x & \text{for } k = -1. \end{cases} \quad (6)$$

Switching to the spatial coordinates (χ, θ, ϕ) , the interval ds^2 can be written as

$$ds^2 = -c^2 dt^2 + a^2(t) [d\chi^2 + \text{sinn}^2 \chi (d\theta^2 + \sin^2 \theta d\phi^2)]. \quad (7)$$

The physical interpretation of χ can be seen by placing ourselves at the origin $r = 0$ and consider a distant, comoving photon emitter in our line-of-sight direction with the coordinate $r = r_e$. Rotate the coordinates so that the direction of the emitter has $\theta = 0, \phi = 0$, we find

$$ds^2 = -c^2 dt^2 + a^2(t) \frac{dr^2}{1 - kr^2} \quad (8)$$

along the line-of-sight. Let t_e be the time of photon emission and t_0 that of its reception. Since light-like worldlines have $ds^2 = 0$, we find, for the photon:

$$\int_{t_e}^{t_0} \frac{cdt}{a(t)} = \int_0^{r_e} \frac{dr}{1 - kr^2} = \chi(r_e). \quad (9)$$

Consider the integrand in the left-hand side of equation (9). The line element $dx = cdt$ is the physical distance the photon has traveled during the time interval dt . But by dividing the physical distance by $a(t)$ we get the comoving distance, therefore χ can be interpreted as the total, integrated comoving distance between the emitter and us. If the spacetime is flat (Euclidean), this comoving distance is just the difference in the radial coordinate $\Delta r = r_e - 0 = r_e$.

Sometimes it is convenient to introduce the *conformal time*, or the *comoving horizon* η as the time component of the four-coordinate. The conformal time is defined as

$$\eta(t) = \int_0^t \frac{dt'}{a(t')} \quad (10)$$

where we integrate from the “beginning of time”. Using $c\eta$ as the time component, the comoving four-coordinate can be written as a dimensionless vector $x^\alpha = (c\eta, \chi, \theta, \phi)$ and the FRW metric takes the form

$$g_{\mu\nu} = a^2(\eta) \begin{pmatrix} -1 & & & \\ & 1 & & \\ & & \text{sinn}^2 \chi & \\ & & & \text{sinn}^2 \chi \sin^2 \theta \end{pmatrix}. \quad (11)$$

B. Expansion, Redshift, and the Hubble parameter

In the introduction we mentioned Hubble’s Law discovered in 1929. Hubble’s original paper had profound impact upon the history of astrophysics and, to a greater extent, mankind’s perception of the universe, but here we only take some time to appreciate two of his timeless insights.

At the end of his paper Hubble briefly discussed the possible mechanisms for “displacements of the spectra” (i.e. redshift, in modern terms) in the de Sitter cosmology model in which the expansion of the universe is dominated by a vacuum energy. He pointed out the two sources of the redshift: the first being “an apparent slowing down of atomic vibrations” and the other attributed to “a general tendency of material particles to scatter”. In today’s words, the first is the special-relativistic effect of Doppler shift caused by the peculiar motion of galaxies, and the latter the general-relativistic, *cosmological redshift* which is linked to the expansion of the comoving grid itself. In the rest of this article we will see how these two effects arise in modern cosmology and end up in our observational figures.

Hubble also noted that his proportional law might be “a first approximation representing a restricted range in distance”, therefore deviating from the pure de Sitter model in which the Hubble constant H should indeed be constant everywhere and throughout the history. This is exactly how we see it now. In the contemporary context, we usually define the *Hubble parameter* H to be the relative expansion rate of the universe:

$$H = \frac{\dot{a}}{a}, \quad (12)$$

and its value is usually expressed in the unit of $\text{km s}^{-1} \text{Mpc}^{-1}$. The Hubble *constant*, H_0 , now officially refers to the current value of the Hubble parameter.

However, it is not apparent how this definition is related to observable quantities. Therefore we have to relate equation (12) to physical observables such as the length, the time, and the redshift.

First, we note that the cosmological redshift z at any time t is related to the scale factor a . Let t_e be the time of a photon’s emission by a distant source and t_0 the time of its reception by an observer “here and now.” The observed redshift z of the source satisfies

$$1 + z = \frac{a(t_0)}{a(t_e)}. \quad (13)$$

Consider an observer who surveys various sources with different redshifts. The ideal survey is assumed to complete instantly — all the observations are done at exactly the same time instance t_0 . Of course this is not strictly true, but we do not expect the scale factor $a(t_0)$ to change “too fast”, and we expect the redshift not to change too much during the temporal scale of our interest (i.e. typical lifetime of humans or observation programs). If we do allow t_0 to change however, we are led to the Sandage-Loeb test [4, 5] that observes the drifting of redshift during a long period of time. Recently, the variation in the apparent magnitude of stable sources over t_0 has also been proposed as a possible cosmological test [6]. To our best knowledge, no data have been produced using these methods by now, and the proposed observation plans usually require ~ 10 years to yield meaningful results [7, 8]. In this paper we will not focus on these methods, and we therefore neglect the passing of t_0 .

We therefore differentiate equation (13) with respect to t_e , setting t_0 as a constant:

$$\frac{da(t_e)}{dt_e} = -\frac{a(t_0)}{(1+z)^2} \frac{dz}{dt_e} = -\frac{a(t_e)}{1+z} \frac{dz}{dt_e}. \quad (14)$$

Dividing both sides by $a(t_e)$ we immediately find

$$H(z) = -\frac{1}{1+z} \frac{dz}{dt_e}. \quad (15)$$

In Section III A, we will see how equation (15) is useful in measuring $H(z)$ by observing passively evolving galaxies.

Another way to relate $H(z)$ to observable quantities is to use the notion of the comoving distance χ introduced in equation (5). Take the time derivative of equation (9), we find

$$\frac{d\chi}{dt_e} = -\frac{c}{a(t_e)}. \quad (16)$$

On the other hand, equation (14) tells us about another derivative dt_e/dz . Therefore we can find the derivative of χ

with respect to the redshift:

$$\begin{aligned} \frac{d\chi}{dz} &= \frac{d\chi}{dt_e} \frac{dt_e}{dz} = \frac{c}{a(t_e)} \frac{a(t_e)}{(1+z)} \frac{dt_e}{da(t_e)} \\ &= \frac{ca(t_e)}{a(t_0)} \frac{dt_e}{da(t_e)} \\ &= \frac{c}{a(t_0)H}, \end{aligned} \quad (17)$$

that is,

$$\frac{d[a(t_0)\chi]}{dz} = \frac{c}{H(z)}. \quad (18)$$

If an observable object spans the length $a(t_0)\Delta\chi$ along the line-of-sight in some redshift slice Δz , we can estimate $H(z)$. But how do we find such objects, i.e. “standard rods”? The idea is not to use the length of a concrete object. Instead, we explore the spatial distribution of matter in the universe and focus on its *statistical* features, such as the peaks in the two-point correlation function of the density field. This is another method for extracting $H(z)$ data from observations. (The quantity $a(t_0)\chi$ can be seen as a distance measure. It is closely related to the “structure distance” $d_S = a(t_0)r$ defined by Weinberg [9, Chapter 8] that naturally arises in calculating the power spectrum of LSS. From equation (5) we can see that the structure distance is equivalent to $a(t_0)\chi$ if the space is flat, or if the object is not too far away.)

III. HUBBLE PARAMETER FROM OBSERVATIONS

Equations (15) and (18) are the bare-bone descriptions of two established methods for $H(z)$ determination: the differential age method and the radial BAO size method respectively. Either has been made possibly only by virtue of state-of-the-art redshift surveys such as the Sloan Digital Sky Survey (SDSS) [10]. In this section, we will review both methods and the data they produced.

A. The Differential Age Method

As equation(15) suggests, to apply age-dating to the expansion history, we look for the variation of ages, Δt , in a redshift bin Δz [11]. The aging of stars serves as an observable indicator of the aging of the universe, because the evolution of stars is a well-studied subject, and stars’ spectra can be taken and analysed to reveal information about their ages. However, at cosmological distance scales it is not practical to observe the stars one by one: we can only take the spectra of galaxies that are ensembles of stars, possibly of different populations. Since different star populations are formed at drastically different epochs, it is important for us to identify galaxies that comprises relatively uniform star populations, and to look for more realistic models of star formation.

The identification of such “clock” galaxies and the observation of their spectra have been carried out for archival data [12], and surveys such as the Gemini Deep Deep Survey (GDDS) [13], VIMOS-VLT Deep Survey (VVDS) and the SDSS [14]. In addition, high-quality spectroscopic data have been acquired from the Keck I telescope for red galaxies in galaxy clusters [15]. Among the galaxies being observed, special notices should be paid to the luminous red galaxies (LRGs). LRGs are massive galaxies whose constituent star populations are fairly homogeneous. They make up a fair proportion in the SDSS sample and, beyond serving as “clocks”, also trace the underlying distribution of matter in the universe (albeit with bias). Therefore, they reveal baryon acoustic oscillation (BAO) signature in the density autocorrelation function that is used as the “standard rod” in the size method.

The identification and spectroscopic observations of these galaxies have led to direct determinations of $H(z)$ in low and intermediate redshift ranges. Jimenez *et al.* [12] first obtained a determination of $H(z) = 69 \pm 12 \text{ km s}^{-1} \text{ Mpc}^{-1}$ at an effective redshift $z \approx 0.09$ by the differential age method. The work was later expanded by Simon *et al.* [16] who extended the determination of $H(z)$ to 8 more redshift bins up to $z \approx 1.8$. This dataset was brought up-to-date by Stern *et al.* [14, Table 2]. Recently, new age-redshift datasets for different galaxy velocity dispersion groups have been made available [17] from SDSS data release (DR) 7 LRG samples. We will see how these data are used in the study of cosmology models in Section IV.

One may wonder why we take the effort to calculate the age differences in redshift bins when the age data themselves can also be used to test cosmological models. The main reason is that the age determination is subjected to systematic errors that can (hopefully) be cancelled out when taking the difference [18]. Of course, we are not gaining anything

for nothing even if the systematics perfectly cancel, for the binning of data lowers the total amount of measurements we can have.

However, recent developments in the study of the formation history of galaxies and their stellar populations have led us to re-consider the assumptions made in previous works. For example, using numerical simulation techniques, Crawford *et al.* [19] have shown that the simple stellar population (SSP) models used in age determination may contribute to the systematic bias that varies across redshift ranges (hence propagating into the differential ages), while models that take the extended star formation history into account can be used to reduce the errors on $H(z)$.

In addition to the complexities in the stellar populations in each galaxy, the heterogeneity of galaxies in the sample also contributes to the errors in $H(z)$ measurements. In [19], new sample selection criteria have been proposed that could help with obtaining more homogeneous galaxy samples for future analyses.

B. The Radial BAO Size Method

In Section II B, we mentioned that the “standard rod” we seek in the sky is not an actual object but a statistical feature. Indeed, the physical sizes of distant celestial objects are usually poorly known. Worse still, even the *apparent*, i.e. angular, sizes of galaxies are ambiguous because galaxies do not show sharp edges, and they appear fuzzy in images. It can be imagined that size measurements along the line-of-sight could only lead to more problems, because even the angular sizes cannot help us much in this case. Therefore, identifying a statistical “standard rod” becomes a necessity.

In the study of LSS, correlation functions are a simple and convenient measure of the statistical features in the spatial distribution of matter in the universe. (For an early yet important treatment of the topic in the context of galaxy surveys, see [20]. For an example of other statistics in the context of BAO, see [21].) The two-point autocorrelation (i.e. the correlation of a density field with itself) function $\xi(\mathbf{r}_1, \mathbf{r}_2)$ is one of the most used member in the correlation function family. It measures the relatedness of position pairs in the same density field: the joint probability of finding two galaxies in volume elements dV_1 and dV_2 located in the neighborhood of spatial positions \mathbf{r}_1 and \mathbf{r}_2 respectively is

$$dP_{12} = n^2 [1 + \xi(\mathbf{r}_1, \mathbf{r}_2)] dV_1 dV_2 \quad (19)$$

where n is the mean number density. If we believe that our universe is homogeneous in a statistical sense (i.e. that the probabilistic distribution, or ensemble, from which the densities anywhere in our particular instance of the universe is drawn, does not vary from one area of the universe to another), the autocorrelation function becomes a function of $\mathbf{r} = \mathbf{r}_1 - \mathbf{r}_2$ only. If we further assume the (statistical) isotropy of the universe, the direction of \mathbf{r} becomes unimportant, and the autocorrelation is dependent on the magnitude of \mathbf{r} only (that is, $\xi = \xi(r)$). Actually, our assumption of homogeneity is unnecessarily strong if we only work with two-point statistics, and all we need is the homogeneity in the first two moments of the underlying ensemble. Such an ensemble is known as a wide-sense stationary (WSS) one.

For a WSS ensemble, the famous Wiener-Khinchin theorem says that the autocorrelation and the power spectrum $P(\mathbf{k})$ form a Fourier transform pair:

$$\begin{aligned} P(k) &= P(\mathbf{k}) = \int \xi(\mathbf{r}) e^{i\mathbf{k}\cdot\mathbf{r}} d^3r, \\ \xi(r) &= \xi(\mathbf{r}) = \frac{1}{(2\pi)^3} \int P(\mathbf{k}) e^{-i\mathbf{k}\cdot\mathbf{r}} d^3k. \end{aligned} \quad (20)$$

(Here we write the power spectrum as $P(k)$, independent of the direction of the wave vector \mathbf{k} , under the same assumption of statistical isotropy mentioned above, but see discussion about redshift distortion below.) Therefore, either the power spectrum or the autocorrelation can serve as a statistical tool to reveal the information contained in the LSS. Methods of estimating $P(k)$ has been developed and the importance of the power spectrum emphasized [22, 23]. On the other hand, for BAO surveys the autocorrelation function is probably a more straightforward way of presenting the results and testing their significance, because the BAO scales manifest themselves as protruding features (“peaks” or “bulges”) in $\xi(r)$. Actually, an estimator to the autocorrelation, along with its variance, can also be conveniently constructed from survey data using pair counts between the survey and random fields [24].

Needless to say, the “true” autocorrelation of the ensemble can never be fully known, because we have only one realization of the random field which is *the* universe we live in. However, *estimating* the autocorrelation still makes sense because for today’s large and well-sampled surveys the assumption of ergodicity is valid, under which the statistics can be performed to infer knowledges about the underlying ensemble [9, Chapter 8 and Appendix D].

Thus, if a random process induces some features in the spatial distribution of matter, the autocorrelation can be numerically computed to reveal such features that are otherwise hidden in the seemingly stochastic distribution. Fur-

thermore, if the mechanism and properties of this process is well understood and quantitatively modelled, parameter estimation using these features becomes a possibility.

One of such possibility is provided by the BAO signatures in the LSS. The mechanism of BAO effects must be traced back to the early universe before recombination, when the Compton scattering rate was much higher than the cosmic expansion rate. Under this extreme limit, the tightly coupled photons and baryons can be treated as a fluid in which the perturbations drive sound waves. The BAO effect in the cosmic microwave background (CMB) radiation has been subjected to extensive theoretical studies (see the early work of Peebles and Yu [25], a powerful analytical treatment by Hu and Sugiyama [26] in Fourier space, another by Bashinsky and Bertschinger [27] in position space, and a review by Hu and Dodelson [28]). It has been confirmed and measured by CMB observations such as the Wilkinson Microwave Anisotropy Probe (WMAP) [29–33]. We will not discuss CMB in detail, and mainly concern ourselves with the aftereffect of BAO, namely its imprints on the large-scale distribution of matter.

The imprints of BAO in the observable distribution of galaxies today was predicted in theory (see [34, 35], and note that these papers were mainly written in the language of $P(k)$ rather than $\xi(r)$). They were first detected in SDSS data by Eisenstein *et al.* [36]. In [37], BAO measurements were made for SDSS and 2dF survey data using the power spectrum, and the results were presented as a general test of cosmological models. The usage of BAO signatures in the LSS as a probe of $H(z)$ was discussed in [38] (see also [39–41]).

The idea of using BAO scales may appear to be simple and straightforward by our description so far, but in reality the autocorrelation function is subjected to various distortion effects that must be accounted for.

First, galaxies are not comoving objects. Their apparent redshifts are inevitably a combined effect of the cosmological redshift and peculiar velocities (which was once contemplated by E. P. Hubble, see Section II B). Peculiar motion distorts the apparent correlation pattern in the redshift space and makes it anisotropic (see [42, 43]). Therefore, the isotropic autocorrelation function $\xi(r)$ fails to be a good measure. In the literature the autocorrelation is usually expressed as a function of scales in the radial (line-of-sight) direction π and transverse direction σ : $\xi = \xi(\sigma, \pi)$ with $r = \sqrt{\sigma^2 + \pi^2}$. The observed $\xi(\sigma, \pi)$ will be a convolution between $\xi(r)$ and the peculiar velocity field.

Second, geometry of the spacetime also distorts the correlation pattern as the observation goes into deeper distances, where the spacetime geometry becomes non-trivial [44]. This is not a major concern for the analyses we will review in the rest of this section, because the survey data were from our local section of the universe ($z \approx 0$), and for $H(z)$ measurements only some thin slices in the redshift space were used. However, future work that deals with deep survey data must take the geometrical distortions into analysis.

There is also the more delicate issue of biasing, meaning that the correlation pattern of the observed “indicators” does not necessarily reflect that of the underlying matter distribution [45]. Among the effects contributing to the bias, the magnification effect by weak lensing is worthy of notice for our discussion, because it has a large effect on the radial autocorrelation function [46, 47].

Using SDSS LRG samples in the redshift range $0.16 \leq z \leq 0.47$, BAO signature was detected in $\xi(\sigma, \pi)$ by Okumura *et al.* [48]. In their work the magnification bias by weak lensing was neglected, but in the redshift range it contributes little to the spherically averaged autocorrelation ξ_0 [46], also known as the monopole:

$$\xi_0(r) = \frac{1}{2} \int_{-1}^1 \xi(\sigma, \pi) d\mu, \quad (21)$$

where $r = \sqrt{\sigma^2 + \pi^2}$, and $\mu = \pi/r$. In [48] the BAO peak was detected in the monopole significantly, while the ridge-like BAO feature was weak in the anisotropic $\xi(\sigma, \pi)$.

Using improved LRG samples from SDSS DRs 6 and 7, and by modelling the weak lensing magnification bias, radial BAO detection and $H(z)$ measurements were made in redshift slices $z = 0.15 \sim 0.30$ and $z = 0.40 \sim 0.47$ by Gaztañaga *et al.* [49] (see Figure 1 for a presentation of the BAO detection). Because these redshift slices were well separated, the two measurements were independent from each other. (In previous works such as [37] the samples overlapped and the results at different z ’s were correlated.)

These $H(z)$ measurements were the first implementation of the radial BAO method. Due to the distortion effects, confirming the significance of the baryon ridge detection becomes a demanding process, since each distortion effect has to be carefully modelled. However, exact modelling of all the distortion effects on all scales is difficult, and when such modelling cannot be done exactly, these effects introduces systematic errors in the measurement of the BAO ridge’s scale.

Despite these, the radial BAO size method still surpasses the age method in precision. In fact, the combined statistical and systematic uncertainties presented an precision of $\sim 4\%$ in $H(z)$ [49, Table 3]. This is intuitively perceptible. As we have seen in Section III A, the age method is affected by the (possibly very large) systematic errors in age determination. Since we can measure spatial quantities of galaxies, i.e. the distribution of their positions, with much greater accuracy than we can do with temporal quantities related to some vaguely defined event (namely the time duration from star formation in the red galaxies to now), one may intuitively expect lower uncertainties from the radial size method than the differential age method.

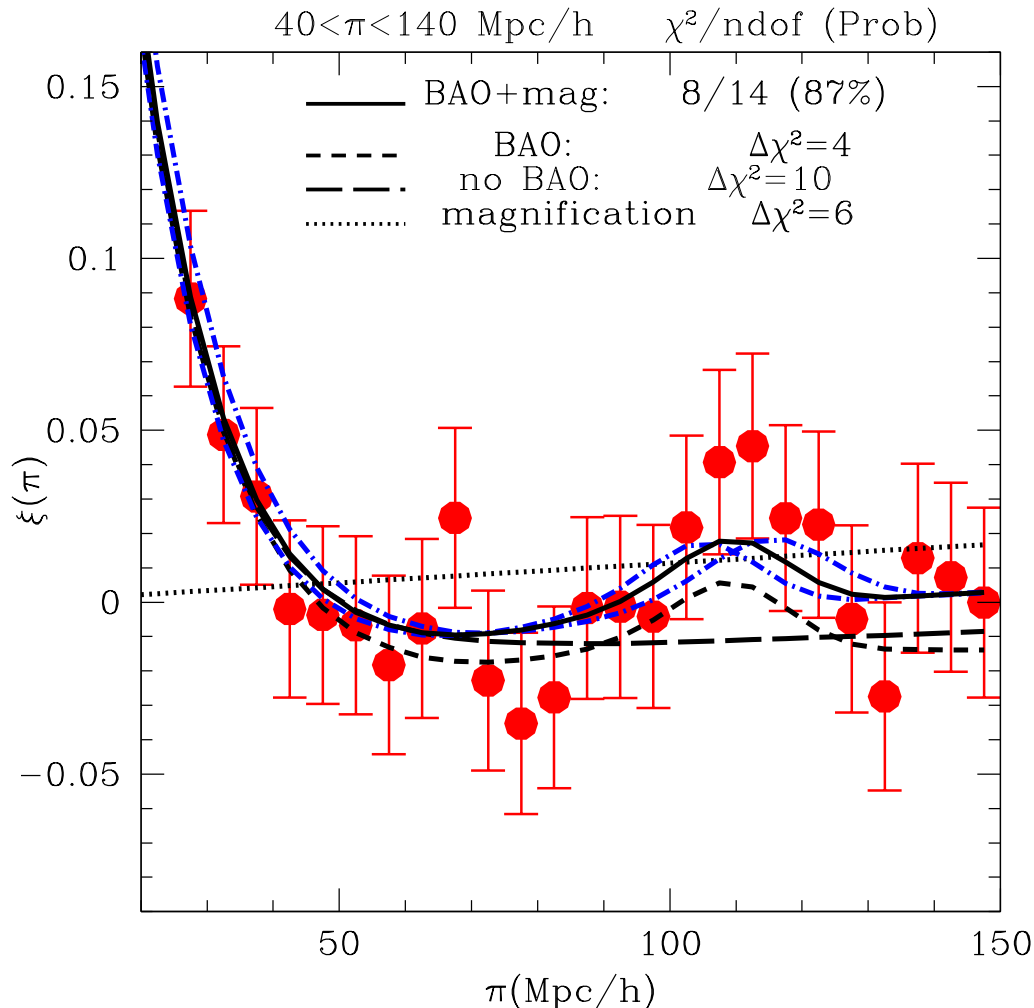


Figure 1. Detection of radial (π -direction) BAO by Gaztañaga *et al.* [49, Figure 13] in the full LRG sample. This is the correlation pattern along the π -direction, and should not be confused with the monopole pattern in Figure 3 of [48]. The effect of weak lensing magnification can be seen by comparing the solid and short dashed curves, which shows that the magnification systematically moves the peak location towards the higher scales. The dash-dotted (blue) curve shows the 1σ range by allowing the fiducial distance-redshift relation used in the analysis to vary in a parameterized way, accounting for the systematic error introduced by the mere using of a fiducial model.

A subtle issue of possible circular logic in the analysis also contributes to the systematic errors in this method. In [49], a fiducial flat Λ CDM model and parameters were used to convert redshifts into distances, and to gauge the comoving BAO scales in the selected redshift slice, r_{BAO} to that of the CMB measured by 5-year WMAP, $r_{\text{WMAP}} = 153.3 \pm 2.0 \text{ Mpc}$ (see [50]) to yield the estimation $H_{\text{BAO}}(z)$:

$$\frac{H_{\text{BAO}}(z)}{r_{\text{BAO}}} = \frac{H_{\text{fid}}(z)}{r_{\text{WMAP}}}, \quad (22)$$

where

$$H_{\text{fid}}(z) = H_0 \sqrt{\Omega_m(1+z)^3 + (1 - \Omega_m)}$$

and $\Omega_m = 0.25$ [51]. The use of a fiducial model introduces bias in all measurements, which is hard to model exactly, but an analysis of this effect was performed using Monte Carlo simulations so that its contribution to the systematic uncertainties could be assessed. The authors of [49] hence argued that the measurement results are model-independent,

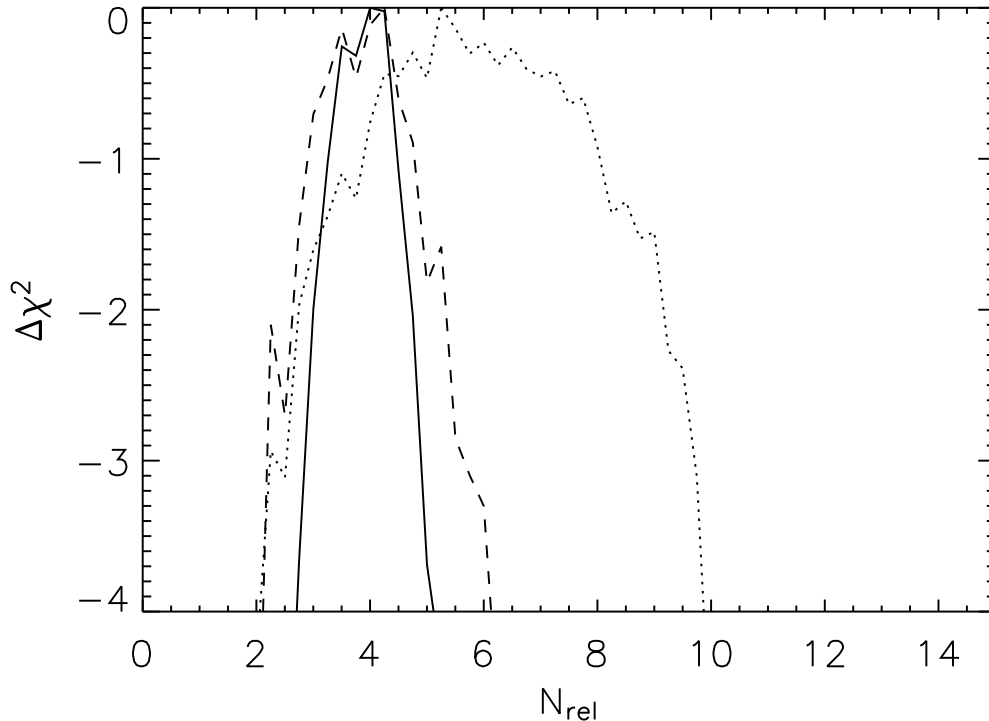


Figure 2. Constraint on the effective number of relativistic species, N_{rel} , by Stern *et al.* [14] using their $H(z)$ measurements by the differential age method. Dotted line plots the 5-year WMAP [54] likelihood, dashed line plots the likelihood with WMAP and H_0 [55], and the solid line plots the likelihood with WMAP, H_0 and $H(z)$ data. The improvement in the constraint by adding $H(z)$ data is evident.

therefore is useful as a general cosmological test. The reader may also consult [37] for a different approach to this issue, using cubic spline fit of the distance-redshift relation so that the result could be applied to a large class of models without having to re-analyze the power spectra for each model to be tested.

IV. OBSERVATIONAL HUBBLE PARAMETER AS A COSMOLOGICAL TEST

The efforts in obtaining observational $H(z)$ data was certainly done with the goal of testing cosmological models in mind. In [12] the observation $H(z)$ at $z \approx 0.09$ was used to constrain the equation of state parameter of dark energy. In [16] the redshift-variability of a slow-roll scalar field dark energy potential was constrained by the differential age $H(z)$ data. The same dataset was also utilized in the study of the Λ CDM universe, especially the summed neutrino masses, the effective number of relativistic species, the spatial curvature, and the dark energy equation of state parameter [52]. The updated $H(z)$ data presented in [14] was used by their authors to improve the results obtained in earlier papers (see Figures 2 and 3 for the application of $H(z)$ data in improving the constraint of the effective number of relativistic species and breaking the degeneracy between spatial curvature and dark energy).

The data produced by the BAO size method in [49] is scarcer in quantity but of higher precision. In [49] they were extrapolated to $z = 0$ to offer an independent estimation of the Hubble constant H_0 , and were used to test the accelerated expansion of the universe. It has been demonstrated that the radial Δz_{BAO} measurements is able to put stringent constraints over the dark energy parameters [53].

In the papers cited above, the parameter constraints obtained from observational $H(z)$ data were shown to be consistent with other cosmological tests, such as the CMB anisotropy. In this way, the observational $H(z)$ data presents themselves as a useful, *independent* cosmological test. In particular, it serves as a powerful tool to break the degeneracy between the curvature and dark energy parameters [52].

These up-to-date data are summarized in Table I. In Figure 4 we plot the $H(z)$ data versus the redshift and compare

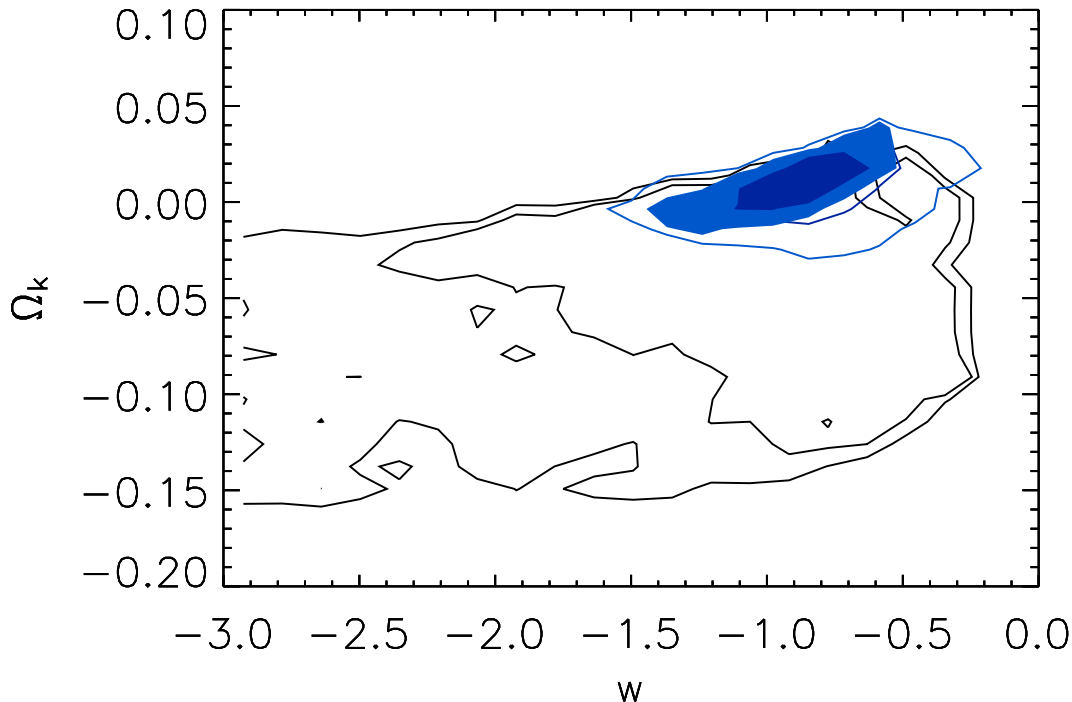


Figure 3. Joint constraint on the energy density corresponding to the spatial curvature, Ω_k , and the dark energy equation of state parameter, w , by Stern *et al.* [14]. The large, irregular regions bounded by dark contours were from 5-year WMAP alone. The blue contours were obtained by adding H_0 constraints. Filled regions were obtained by further adding $H(z)$ data. The application of $H(z)$ data helps with breaking the degeneracy between Ω_k and w .

them with the fiducial spatially flat Λ CDM model with $\Omega_m = 0.25$, $\Omega_\Lambda = 0.75$, and $H_0 = 72 \text{ km s}^{-1} \text{ Mpc}^{-1}$.

In addition to the above authors, the observational $H(z)$ datasets have been widely used to put various cosmological models under test. The first adopters included Yi and Zhang [56] and Samushia and Ratra [57] who made use of the $H(z)$ results of [16] in the study of dark energy. In [56] the $H(z)$ data alone were used to constrain the parameters of the holographic dark energy model, especially the c parameter that determines the dynamical history of the expanding universe (see Figure 5). The updated data in [14] and [49] have also been adopted to constrain the parameters in more exotic dark energy models, e.g. [58, 59].

Beyond parameter constraints, the observational $H(z)$ data are also applicable in non-parametric, model-independent cosmological tests. For example, the Om statistic by Sahni *et al.* [60], defined by

$$Om(z) = \frac{h^2(z) - 1}{(1+z)^3 - 1}, \quad (23)$$

where h is the dimensionless Hubble parameter, $h = H(z)/H_0$. This statistic is useful as a null test of dark energy being a cosmological constant Λ , and is more robust than parameterizations of the dark energy equation of state. In [60] however, the Hubble parameter used were not the independent observational data discussed in this review, but the ones reconstructed using SNIa luminosity distance data. In a subsequent paper [61], these independent, observational $H(z)$ data found their way into the non-parametric test, and they further played roles in other model-independent diagnostics that could test the spatial flatness of the universe, or even the homogeneity assumed by the FRW metric (2).

Despite the wide application of the $H(z)$ datasets in the literature, we would like to point out some issues associated with their usage.

First, in some papers [58, 59, 62] that made use of $H(z)$ data derived from radial BAO by Gaztañaga *et al.* [49] in χ^2 analyses, the measurement at a middle redshift $z = 0.34$ was used in conjunction with those from the two independent redshift slices near $z = 0.24$ and 0.43 , under the tacit assumption of being independent from each other. However, this

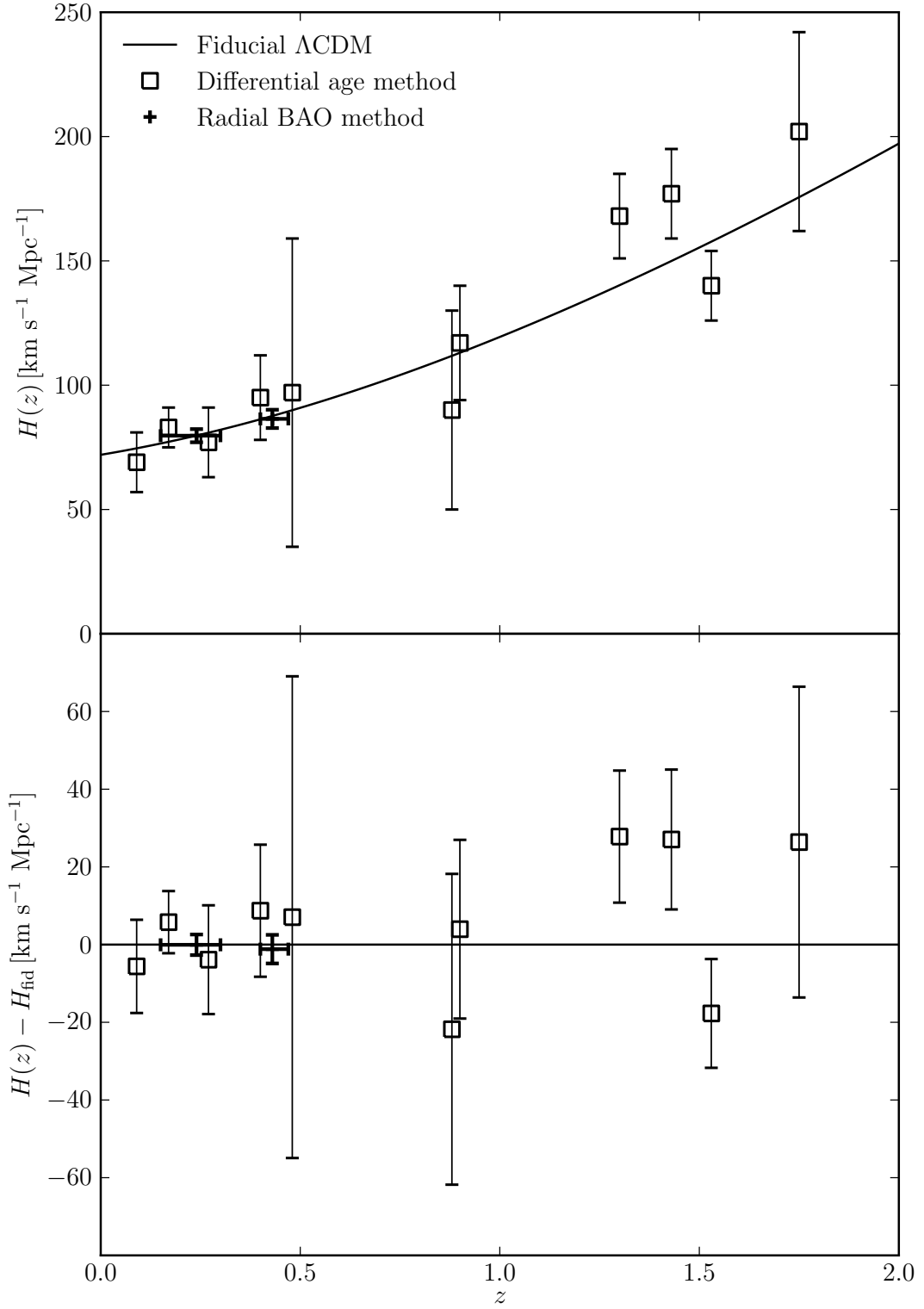


Figure 4. Top panel — the available $H(z)$ data from both differential age method and radial BAO size method (see Table I and references therein). The solid curve plots the theoretical Hubble parameter H_{fid} as a function of z from the fiducial ΛCDM model with $\Omega_{\text{m}} = 0.25, \Omega_{\Lambda} = 0.75$, and $H_0 = 72 \text{ km s}^{-1} \text{Mpc}^{-1}$. Bottom panel — the same data, but the residuals with respect to the fiducial model H_{fid} are plotted. In both panels, the z error bars on the measurements from the radial BAO method are used to mark the extents of the two independent redshift slices in which the BAO peaks were measured.

Table I. The set of available observational $H(z)$ data

z	$H(z) \pm 1\sigma$ error ^a	References	Remarks
0.09	69 ± 12	[12, 14]	
0.17	83 ± 8	[14]	
0.24	79.69 ± 2.65^b	[49]	In the redshift slice $0.15 \sim 0.30$
0.27	77 ± 14	[14]	
0.4	95 ± 17	[14]	
0.43	86.45 ± 3.68^b	[49]	In the redshift slice $0.40 \sim 0.47$
0.48	97 ± 62	[14]	
0.88	90 ± 40	[14]	
0.9	117 ± 23	[14]	
1.3	168 ± 17	[14]	
1.43	177 ± 18	[14]	
1.53	140 ± 14	[14]	
1.75	202 ± 40	[14]	

^a $H(z)$ figures are in the unit of $\text{km s}^{-1} \text{Mpc}^{-1}$.

^b Including both statistical and systematic uncertainties: $\sigma = \sqrt{\sigma_{\text{sta}}^2 + \sigma_{\text{sys}}^2}$.

is not true, because the determination at the middle redshift was not made from a separate, non-overlapping redshift slice, but from the whole sample of galaxies, *including* the lower and upper redshift ranges. If the data is to be used in quantitative works, this interdependency should not be ignored and must be explicitly analysed. A related issue is combining the $H(z)$ data determined from radial BAO peaks with the Δz_{BAO} data derived using the same method under the assumption of their independence (this practice can be found, for example, in [62]). To be rigorous (or pedantic, depending on your point of view), we do not believe that this is the best way to use the data, and we insist on an analysis involving the (non-diagonal) covariance between these datasets. On the other hand, the combination of Δz_{BAO} data and *age*-dated $H(z)$ is mostly free from this interdependence problem, and they actually complement each other well [63, in particular Figures 1 and 2]. We also note that in qualitative explorations one may choose to relax this restriction to some reasonable extent, for example in the discussion of accelerate expansion in [49, Section 4.4].

Another topic that could be worthy of future discussions is the possible tension between the $H(z)$ datasets and other observational data. As noted by Figueroa *et al.* [52], datasets of different physical natures and systematic effects can be safely combined only if they agree with each other well (see also [64]). In this regard, we note that there is possibly some tension between $H(z)$ and type Ia supernova (SNIa) luminosity distances as shown in [63] (see Figure 6). However, this apparent tension could be statistical in nature and may simply be a consequence of not having enough independent measurements of $H(z)$. We hope that future expanded $H(z)$ datasets would allow us to check its consistency with other data in a quantitative manner.

V. FUTURE DIRECTIONS

The available $H(z)$ data have so far proven to be a useful tool in the pursuit of understanding the expansion history of the universe and the possible nature of dark energy. However, these datasets do not have very good redshift coverage. The current measurements have gone as deep as $z = 1.75$, and this redshift range is only sparsely covered. There is also another issue of the large error bars associated with the $H(z)$ figures from the differential age method. On the other hand, the collection of more and higher quality $H(z)$ data will not only help us constrain the parameters, but will also allow us to understand the possible tension between $H(z)$ and other cosmological tests. The latter is important, because tension is usually an indicator of systematic errors in the data. By understanding the tension, we may finally conquer the systematic effects that have not yet been modelled well enough.

In this section, we will describe a few directions of future cosmological observations and their implications in the measurements of the Hubble parameter.

A. Future Improvements in the Differential Age Method

The relatively large uncertainties in the differential age method could be partially compensated if future datasets could offer better coverage in the redshift range accessible by this method. Using mock data, we recently estimated

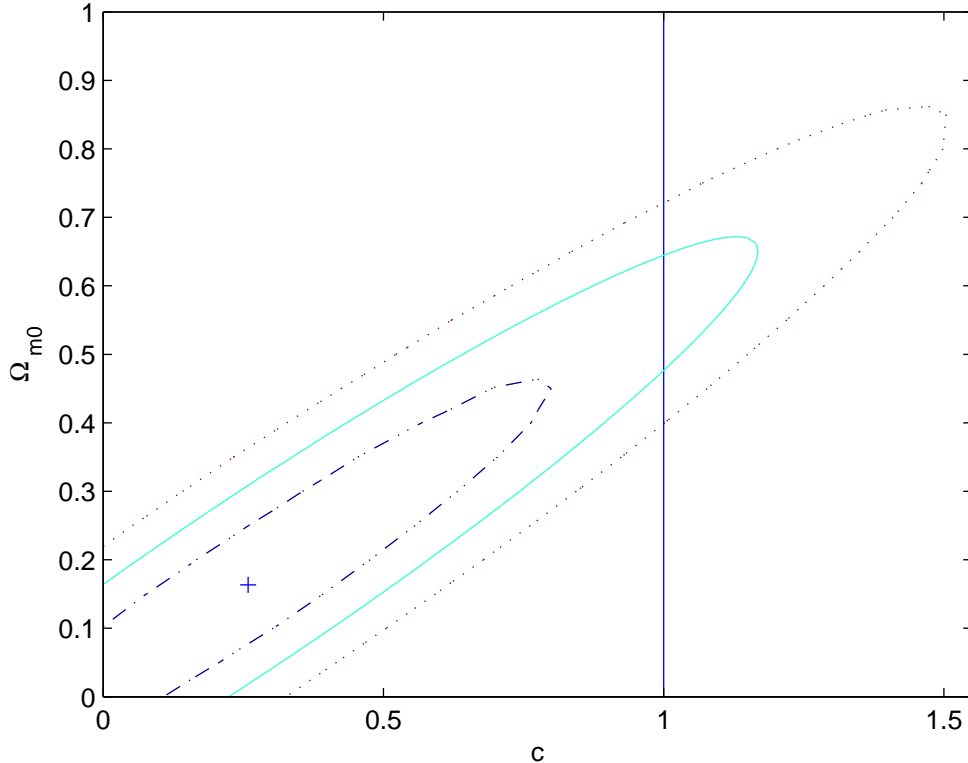


Figure 5. Parameter constraints for the holographic dark energy model in the Ω_m - c plane, by Yi and Zhang [56]. The constraints were obtained using age-determined $H(z)$ data in [16] alone. The cross in the lower-left marks the best-fit value. The dash-dotted, solid, and dotted contours marks the 68.3%, 95.4%, and 99.7% confidence regions respectively. Although some degeneracy exists, it is evident that the data favor models with $c < 1$.

that future $H(z)$ datasets would offer similar or even higher parameter-constraining power compared with current SNIa datasets if it could add as many as ~ 60 independent measurements to cover the redshift range $0 \leq z \leq 2$ [66]. To achieve this level of data coverage, future surveys must be able to offer a large sample of LRGs to be used in age-dating. According to [16], the Atacama Cosmology Telescope (ACT) [67] can be utilized in the future to identify passively evolving, red galaxies by their Sunyaev-Zel'dovich effect. These galaxies can in turn be spectroscopically measured and age-dated, and it has been estimated that they could yield ~ 1000 $H(z)$ measurements. This means the quality of current differential age $H(z)$ data can be expected to increase significantly.

The error model used in the analysis of differential age $H(z)$ data in [66] was empirical, which may have underestimated possible future improvements. In [19] it has been estimated that $H(z)$ may be measured within 3% relative error at $z \approx 0.42$ in realistic observations if the star formation systematics could be properly accounted for. This level of precision is on par with the current status of the radial BAO method, and we hope it could be achieved in the near future.

B. Future Improvements in the Radial BAO Size Method

The radial BAO size method has already been demonstrated to provide highly accurate $H(z)$ measurements. However, this accuracy came at a cost, for spectroscopic data must be taken for the great number of galaxies under survey to find their redshifts, which is time-consuming. Fortunately it turns out that for low redshift ranges, photometric redshift surveys can be a sufficient and promising approach [68–70] to the detection and measurements of radial BAO features in the autocorrelation function. Photometry has several advantages over spectroscopy – it is cheaper, faster, and able to reach fainter sources.

The BAO method is unique in that it allows us to reconstruct the cosmic expansion through a vast range of eras. Unlike the differential age method in which the observable indicators of time are located within a limited redshift

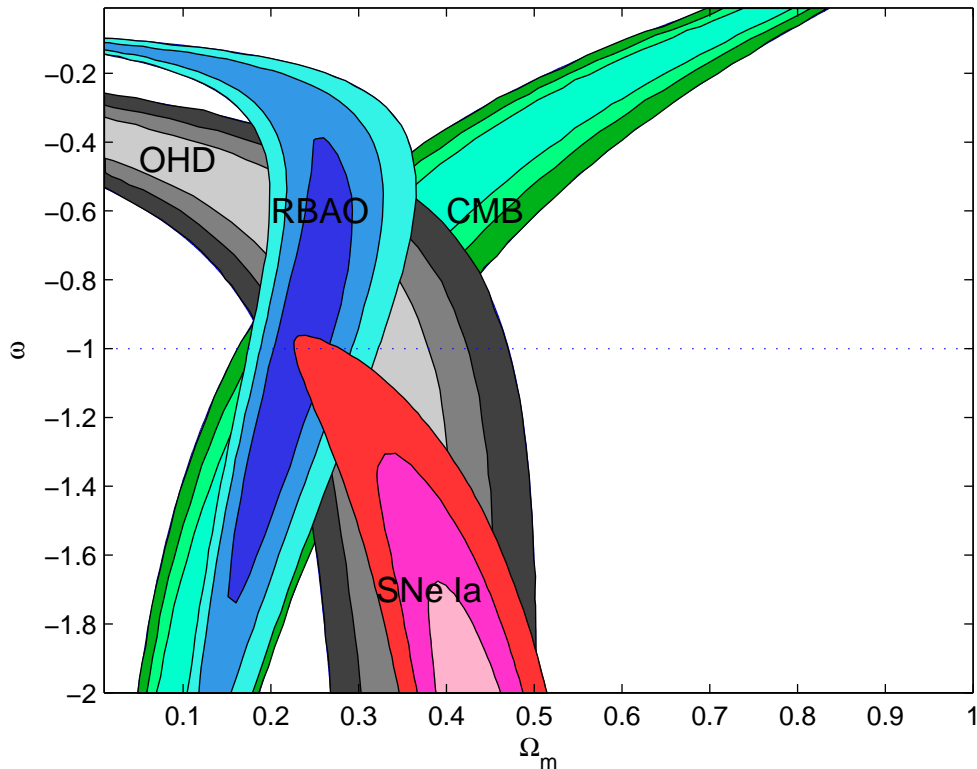


Figure 6. Possible tension between $H(z)$ and type Ia supernovae data depicted in the χ^2 fitting results for the spatially flat XCDM model (similar to Λ CDM, except that the dark energy equation of state parameter ω is set free instead of being fixed at $\omega = -1$). The SN data favor a phantom dark energy with $\omega < -1$ while other data, including observational $H(z)$ (OHD), are consistent with Λ CDM. The OHD used in this figure were the measurements by [16] using the differential age method, and the SN data were from [65]. The RBAO contours were found using the Δz_{BAO} data in [49]. Confidence regions are 68.3%, 95.4%, and 99.7% respectively. This figure first appeared in [63, Fig. 4].

range, BAO signal detection is possible as long as the distribution of matter, regardless of its form, can be traced. Even if the current implementation of the radial BAO method is mainly confined in the redshift range of $z \approx 0$, future redshift surveys such as the planned SDSS III project [71] are designed to reach into deeper universe and measure $H(z)$ at redshifts up to $z \approx 2.5$ by observing the Lyman- α forest absorption spectra of high-redshift quasars (see [72] for a discussion of high- z measurement of radial BAO and $H(z)$ and its implication for dark energy, and [73, 74] for numerical simulation studies). Recently, the enormous potential of space-based redshift surveys in the determination of $H(z)$ and other parameters has been studied in [75]. Moreover, the proposed observational programs of the 21 cm background may further extend our knowledge of $H(z)$ into even deeper redshift ranges before or near the reionization era [76–78], the “dark ages” that have not been extensively explored by current observations yet.

VI. SUMMARY

In this paper, we reviewed the current status of observationally measured Hubble parameter data. We presented the principle ideas behind the two important and independent methods of $H(z)$ measurement, namely the differential age method and the radial BAO size method. Both methods have been successfully implemented over the years to yield $H(z)$ data that are of varying precision and redshift coverage, and the up-to-date results have been summarized in Table I. These data are valuable for the study of the expanding universe. They have seen wide application by cosmologists to put various cosmological models under test, and to constrain important cosmological parameters either independently or in conjunction with data of different physical natures. However, we also pointed out several issues in the usage of observational $H(z)$ data. Finally, despite some current shortcomings, we find the $H(z)$ data of great potential, as future observational programs can be expected to improve significantly the quality of $H(z)$ data

that may lead us into unexplored realms of the universe.

ACKNOWLEDGMENTS

We would like to thank Zhongfu Yu for his help in preparing some of the materials in the bibliography list. This work was supported by the National Science Foundation of China (Grants No. 10473002), the Ministry of Science and Technology National Basic Science program (project 973) under grant No. 2009CB24901, Scientific Research Foundation of Beijing Normal University and the Scientific Research Foundation for the Returned Overseas Chinese Scholars, State Education Ministry.

-
- [1] E. P. Hubble, “A relation between distance and radial velocity among extra-galactic nebulae,” *Proc. Natl. Acad. Sci. USA*, **15**, 168–173 (1929).
 - [2] A. G. Riess, A. V. Filippenko, P. Challis, A. Clocchiatti, A. Diercks, P. M. Garnavich, R. L. Gilliland, C. J. Hogan, S. Jha, R. P. Kirshner, B. Leibundgut, M. M. Phillips, D. Reiss, B. P. Schmidt, R. A. Schommer, R. C. Smith, J. Spyromilio, C. Stubbs, N. B. Suntzeff, and J. Tonry, “Observational evidence from supernovae for an accelerating universe and a cosmological constant,” *AJ*, **116**, 1009–1038 (1998), arXiv:astro-ph/9805201.
 - [3] S. Perlmutter, G. Aldering, G. Goldhaber, R. A. Knop, P. Nugent, P. G. Castro, S. Deustua, S. Fabbro, A. Goobar, D. E. Groom, I. M. Hook, A. G. Kim, M. Y. Kim, J. C. Lee, N. J. Nunes, R. Pain, C. R. Pennypacker, R. Quimby, C. Lidman, R. S. Ellis, M. Irwin, R. G. McMahon, P. Ruiz-Lapuente, N. Walton, B. Schaefer, B. J. Boyle, A. V. Filippenko, T. Matheson, A. S. Fruchter, N. Panagia, H. J. M. Newberg, W. J. Couch, and The Supernova Cosmology Project, “Measurements of Ω and Λ from 42 high-redshift supernovae,” *ApJ*, **517**, 565–586 (1999), arXiv:astro-ph/9812133.
 - [4] A. Sandage, “The change of redshift and apparent luminosity of galaxies due to the deceleration of selected expanding universes,” *ApJ*, **136**, 319–333 (1962).
 - [5] A. Loeb, “Direct measurement of cosmological parameters from the cosmic deceleration of extragalactic objects,” *ApJ*, **499**, L111–L114 (1998), arXiv:astro-ph/9802112.
 - [6] S. Qi and T. Lu, “Possible direct measurement of the expansion rate of the universe,” preprint (2010), arXiv:1001.3975 [astro-ph.CO].
 - [7] P.-S. Corasaniti, D. Huterer, and A. Melchiorri, “Exploring the dark energy redshift desert with the Sandage-Loeb test,” *Phys. Rev. D*, **75**, 062001 (2007), arXiv:astro-ph/0701433.
 - [8] J. Zhang, L. Zhang, and X. Zhang, “Sandage-Loeb test for the new agegraphic and Ricci dark energy models,” *Physics Letters B*, **691**, 11–17 (2010), arXiv:1006.1738 [astro-ph.CO].
 - [9] S. Weinberg, *Cosmology* (Oxford Univ. Press Inc., New York, 2008) ISBN 978-0-19-852682-7.
 - [10] <http://www.sdss.org/>.
 - [11] R. Jimenez and A. Loeb, “Constraining cosmological parameters based on relative galaxy ages,” *ApJ*, **573**, 37–42 (2002), arXiv:astro-ph/0106145.
 - [12] R. Jimenez, L. Verde, T. Treu, and D. Stern, “Constraints on the equation of state of dark energy and the Hubble constant from stellar ages and the cosmic microwave background,” *ApJ*, **593**, 622–629 (2003), arXiv:astro-ph/0302560.
 - [13] P. J. McCarthy, D. Le Borgne, D. Crampton, H.-W. Chen, R. G. Abraham, K. Glazebrook, S. Savaglio, R. G. Carlberg, R. O. Marzke, K. Roth, I. Jørgensen, I. Hook, R. Murowinski, and S. Juneau, “Evolved galaxies at $z > 1.5$ from the Gemini Deep Deep Survey: The formation epoch of massive stellar systems,” *ApJ*, **614**, L9–L12 (2004), arXiv:astro-ph/0408367.
 - [14] D. Stern, R. Jimenez, L. Verde, M. Kamionkowski, and S. A. Stanford, “Cosmic chronometers: constraining the equation of state of dark energy. I: $H(z)$ measurements,” *Journal of Cosmology and Astro-Particle Physics*, **2**, 8 (2010), arXiv:0907.3149 [astro-ph.CO].
 - [15] D. Stern, R. Jimenez, L. Verde, S. A. Stanford, and M. Kamionkowski, “Cosmic chronometers: Constraining the equation of state of dark energy. II: A spectroscopic catalog of red galaxies in galaxy clusters,” *ApJS*, **188**, 280–289 (2010), arXiv:0907.3152 [astro-ph.CO].
 - [16] J. Simon, L. Verde, and R. Jimenez, “Constraints on the redshift dependence of the dark energy potential,” *Phys. Rev. D*, **71**, 123001 (2005), arXiv:astro-ph/0412269.
 - [17] D. P. Carson and R. C. Nichol, “The age-redshift relation for luminous red galaxies in the Sloan Digital Sky Survey,” *MNRAS*, in press (2010), arXiv:1006.2830 [astro-ph.CO].
 - [18] R. Jimenez, J. MacDonald, J. S. Dunlop, P. Padoan, and J. A. Peacock, “Synthetic stellar populations: single stellar populations, stellar interior models and primordial protogalaxies,” *MNRAS*, **349**, 240–254 (2004), arXiv:astro-ph/0402271.
 - [19] S. M. Crawford, A. L. Ratsimbazafy, C. M. Cress, E. A. Olivier, S.-L. Blyth, and K. J. van der Heyden, “Luminous red galaxies in simulations: cosmic chronometers?” *MNRAS*, 1026 (2010), arXiv:1004.2378 [astro-ph.CO].
 - [20] P. J. E. Peebles, “Statistical analysis of catalogs of extragalactic objects. I. Theory,” *ApJ*, **185**, 413–440 (1973), the term *covariance function* used in this article is also known as the *correlation function* which occurs more frequently in the contemporary literature.

- [21] X. Xu, M. White, N. Padmanabhan, D. J. Eisenstein, J. Eckel, K. Mehta, M. Metchnik, P. Pinto, and H.-J. Seo, “A new statistic for analyzing baryon acoustic oscillations,” *ApJ*, **718**, 1224–1234 (2010), arXiv:1001.2324 [astro-ph.CO].
- [22] H. A. Feldman, N. Kaiser, and J. A. Peacock, “Power-spectrum analysis of three-dimensional redshift surveys,” *ApJ*, **426**, 23–37 (1994), arXiv:astro-ph/9304022.
- [23] W. J. Percival, L. Verde, and J. A. Peacock, “Fourier analysis of luminosity-dependent galaxy clustering,” *MNRAS*, **347**, 645–653 (2004), arXiv:astro-ph/0306511.
- [24] S. D. Landy and A. S. Szalay, “Bias and variance of angular correlation functions,” *ApJ*, **412**, 64–71 (1993).
- [25] P. J. E. Peebles and J. T. Yu, “Primeval adiabatic perturbation in an expanding universe,” *ApJ*, **162**, 815–836 (1970).
- [26] W. Hu and N. Sugiyama, “Anisotropies in the cosmic microwave background: an analytic approach,” *ApJ*, **444**, 489–506 (1995), arXiv:astro-ph/9407093.
- [27] S. Bashinsky and E. Bertschinger, “Dynamics of cosmological perturbations in position space,” *Phys. Rev. D*, **65**, 123008 (2002), arXiv:astro-ph/0202215.
- [28] W. Hu and S. Dodelson, “Cosmic microwave background anisotropies,” *ARA&A*, **40**, 171–216 (2002), arXiv:astro-ph/0110414.
- [29] G. Hinshaw, D. N. Spergel, L. Verde, R. S. Hill, S. S. Meyer, C. Barnes, C. L. Bennett, M. Halpern, N. Jarosik, A. Kogut, E. Komatsu, M. Limon, L. Page, G. S. Tucker, J. L. Weiland, E. Wollack, and E. L. Wright, “First-year Wilkinson Microwave Anisotropy Probe (WMAP) observations: The angular power spectrum,” *ApJS*, **148**, 135–159 (2003), arXiv:astro-ph/0302217.
- [30] L. Page, M. R. Nolta, C. Barnes, C. L. Bennett, M. Halpern, G. Hinshaw, N. Jarosik, A. Kogut, M. Limon, S. S. Meyer, H. V. Peiris, D. N. Spergel, G. S. Tucker, E. Wollack, and E. L. Wright, “First-year Wilkinson Microwave Anisotropy Probe (WMAP) observations: Interpretation of the TT and TE angular power spectrum peaks,” *ApJS*, **148**, 233–241 (2003), arXiv:astro-ph/0302220.
- [31] G. Hinshaw, M. R. Nolta, C. L. Bennett, R. Bean, O. Doré, M. R. Greason, M. Halpern, R. S. Hill, N. Jarosik, A. Kogut, E. Komatsu, M. Limon, N. Odegard, S. S. Meyer, L. Page, H. V. Peiris, D. N. Spergel, G. S. Tucker, L. Verde, J. L. Weiland, E. Wollack, and E. L. Wright, “Three-year Wilkinson Microwave Anisotropy Probe (WMAP) observations: Temperature analysis,” *ApJS*, **170**, 288–334 (2007), arXiv:astro-ph/0603451.
- [32] M. R. Nolta, J. Dunkley, R. S. Hill, G. Hinshaw, E. Komatsu, D. Larson, L. Page, D. N. Spergel, C. L. Bennett, B. Gold, N. Jarosik, N. Odegard, J. L. Weiland, E. Wollack, M. Halpern, A. Kogut, M. Limon, S. S. Meyer, G. S. Tucker, and E. L. Wright, “Five-year Wilkinson Microwave Anisotropy Probe observations: Angular power spectra,” *ApJS*, **180**, 296–305 (2009), arXiv:0803.0593.
- [33] D. Larson, J. Dunkley, G. Hinshaw, E. Komatsu, M. R. Nolta, C. L. Bennett, B. Gold, M. Halpern, R. S. Hill, N. Jarosik, A. Kogut, M. Limon, S. S. Meyer, N. Odegard, L. Page, K. M. Smith, D. N. Spergel, G. S. Tucker, J. L. Weiland, E. Wollack, and E. L. Wright, “Seven-year Wilkinson Microwave Anisotropy Probe (WMAP) observations: Power spectra and WMAP-derived parameters,” *ApJS*, in press (2010), arXiv:1001.4635 [astro-ph.CO].
- [34] D. M. Goldberg and M. A. Strauss, “Determination of the baryon density from large-scale galaxy redshift surveys,” *ApJ*, **495**, 29–43 (1998), arXiv:astro-ph/9707209.
- [35] A. Meiksin, M. White, and J. A. Peacock, “Baryonic signatures in large-scale structure,” *MNRAS*, **304**, 851–864 (1999), arXiv:astro-ph/9812214.
- [36] D. J. Eisenstein, I. Zehavi, D. W. Hogg, R. Scoccimarro, M. R. Blanton, R. C. Nichol, R. Scranton, H.-J. Seo, M. Tegmark, Z. Zheng, S. F. Anderson, J. Annis, N. Bahcall, J. Brinkmann, S. Burles, F. J. Castander, A. Connolly, I. Csabai, M. Doi, M. Fukugita, J. A. Frieman, K. Glazebrook, J. E. Gunn, J. S. Hendry, G. Hennessy, Z. Ivezić, S. Kent, G. R. Knapp, H. Lin, Y.-S. Loh, R. H. Lupton, B. Margon, T. A. McKay, A. Meiksin, J. A. Munn, A. Pope, M. W. Richmond, D. Schlegel, D. P. Schneider, K. Shimasaku, C. Stoughton, M. A. Strauss, M. SubbaRao, A. S. Szalay, I. Szapudi, D. L. Tucker, B. Yanny, and D. G. York, “Detection of the baryon acoustic peak in the large-scale correlation function of SDSS luminous red galaxies,” *ApJ*, **633**, 560–574 (2005), arXiv:astro-ph/0501171.
- [37] W. J. Percival, S. Cole, D. J. Eisenstein, R. C. Nichol, J. A. Peacock, A. C. Pope, and A. S. Szalay, “Measuring the baryon acoustic oscillation scale using the Sloan Digital Sky Survey and 2dF Galaxy Redshift Survey,” *MNRAS*, **381**, 1053–1066 (2007), arXiv:0705.3323.
- [38] H.-J. Seo and D. J. Eisenstein, “Probing dark energy with baryonic acoustic oscillations from future large galaxy redshift surveys,” *ApJ*, **598**, 720–740 (2003), arXiv:astro-ph/0307460.
- [39] C. Blake and K. Glazebrook, “Probing dark energy using baryonic oscillations in the galaxy power spectrum as a cosmological ruler,” *ApJ*, **594**, 665–673 (2003), arXiv:astro-ph/0301632.
- [40] H.-J. Seo and D. J. Eisenstein, “Baryonic acoustic oscillations in simulated galaxy redshift surveys,” *ApJ*, **633**, 575–588 (2005), arXiv:astro-ph/0507338.
- [41] H.-J. Seo and D. J. Eisenstein, “Improved forecasts for the baryon acoustic oscillations and cosmological distance scale,” *ApJ*, **665**, 14–24 (2007), arXiv:astro-ph/0701079.
- [42] M. Davis and P. J. E. Peebles, “A survey of galaxy redshifts. V - The two-point position and velocity correlations,” *ApJ*, **267**, 465–482 (1983).
- [43] N. Kaiser, “Clustering in real space and in redshift space,” *MNRAS*, **227**, 1–21 (1987).
- [44] H. Magira, Y. P. Jing, and Y. Suto, “Cosmological redshift-space distortion on clustering of high-redshift objects: Correction for nonlinear effects in the power spectrum and tests with N -body simulations,” *ApJ*, **528**, 30–50 (2000), arXiv:astro-ph/9907438.
- [45] N. Kaiser, “On the spatial correlations of Abell clusters,” *ApJ*, **284**, L9–L12 (1984).

- [46] L. Hui, E. Gaztañaga, and M. Loverde, “Anisotropic magnification distortion of the 3D galaxy correlation. I. Real space,” *Phys. Rev. D*, **76**, 103502 (2007), arXiv:0706.1071.
- [47] L. Hui, E. Gaztañaga, and M. Loverde, “Anisotropic magnification distortion of the 3D galaxy correlation. II. Fourier and redshift space,” *Phys. Rev. D*, **77**, 063526 (2008), arXiv:0710.4191.
- [48] T. Okumura, T. Matsubara, D. J. Eisenstein, I. Kayo, C. Hikage, A. S. Szalay, and D. P. Schneider, “Large-scale anisotropic correlation function of SDSS luminous red galaxies,” *ApJ*, **676**, 889–898 (2008), arXiv:0711.3640.
- [49] E. Gaztañaga, A. Cabré, and L. Hui, “Clustering of luminous red galaxies - IV. Baryon acoustic peak in the line-of-sight direction and a direct measurement of $H(z)$,” *MNRAS*, **399**, 1663–1680 (2009), arXiv:0807.3551.
- [50] E. Komatsu, J. Dunkley, M. R. Nolte, C. L. Bennett, B. Gold, G. Hinshaw, N. Jarosik, D. Larson, M. Limon, L. Page, D. N. Spergel, M. Halpern, R. S. Hill, A. Kogut, S. S. Meyer, G. S. Tucker, J. L. Weiland, E. Wollack, and E. L. Wright, “Five-year Wilkinson Microwave Anisotropy Probe Observations: Cosmological interpretation,” *ApJS*, **180**, 330–376 (2009), arXiv:0803.0547.
- [51] Another way to present the measurement results for use in cosmological parameter constraint $\Delta z_{\text{BAO}} = r_{\text{BAO}} H(z)/c$. Schematically, this is done by approximating the derivative in equation (18) with a ratio of differences, and identifying the interval $a(t_0)\Delta\chi$ with the measured comoving BAO scale. In Section IV we briefly discuss its usage.
- [52] D. G. Figueroa, L. Verde, and R. Jimenez, “Improved cosmological parameter constraints from CMB and $H(z)$ data,” *Journal of Cosmology and Astro-Particle Physics*, **10**, 38 (2008), arXiv:0807.0039.
- [53] E. Gaztañaga, R. Miquel, and E. Sánchez, “First cosmological constraints on dark energy from the radial baryon acoustic scale,” *Phys. Rev. Lett.*, **103**, 091302 (2009), arXiv:0808.1921.
- [54] J. Dunkley, E. Komatsu, M. R. Nolte, D. N. Spergel, D. Larson, G. Hinshaw, L. Page, C. L. Bennett, B. Gold, N. Jarosik, J. L. Weiland, M. Halpern, R. S. Hill, A. Kogut, M. Limon, S. S. Meyer, G. S. Tucker, E. Wollack, and E. L. Wright, “Five-year Wilkinson Microwave Anisotropy Probe observations: Likelihoods and parameters from the WMAP data,” *ApJS*, **180**, 306–329 (2009), arXiv:0803.0586.
- [55] A. G. Riess, L. Macri, S. Casertano, M. Sosey, H. Lampeitl, H. C. Ferguson, A. V. Filippenko, S. W. Jha, W. Li, R. Chornock, and D. Sarkar, “A redetermination of the Hubble constant with the Hubble Space Telescope from a differential distance ladder,” *ApJ*, **699**, 539–563 (2009), arXiv:0905.0695.
- [56] Ze-Long Yi and Tong-Jie Zhang, “Constraints on holographic dark energy models using the differential ages of passively evolving galaxies,” *Mod. Phys. Lett. A*, **22**, 41–53 (2007), arXiv:astro-ph/0605596.
- [57] L. Samushia and B. Ratra, “Cosmological constraints from Hubble parameter versus redshift data,” *ApJ*, **650**, L5–L8 (2006), arXiv:astro-ph/0607301.
- [58] L. Xu and Y. Wang, “Observational constraints to Ricci dark energy model by using: SN, BAO, OHD, fgas data sets,” *Journal of Cosmology and Astro-Particle Physics*, **6**, 2 (2010), arXiv:1006.0296 [astro-ph.CO].
- [59] I. Durán, D. Pavón, and W. Zimdahl, “Observational constraints on a holographic, interacting dark energy model,” *Journal of Cosmology and Astro-Particle Physics*, **7**, 18 (2010), arXiv:1007.0390 [astro-ph.CO].
- [60] V. Sahni, A. Shafieloo, and A. A. Starobinsky, “Two new diagnostics of dark energy,” *Phys. Rev. D*, **78**, 103502 (2008), arXiv:0807.3548.
- [61] A. Shafieloo and C. Clarkson, “Model independent tests of the standard cosmological model,” *Phys. Rev. D*, **81**, 083537 (2010), arXiv:0911.4858 [astro-ph.CO].
- [62] N. Pan, Y. Gong, Y. Chen, and Z.-H. Zhu, “Improved cosmological constraints on the curvature and equation of state of dark energy,” *Class. Quantum Grav.*, **27**, 155015 (2010), arXiv:1005.4249 [astro-ph.CO].
- [63] Z.-X. Zhai, H.-Y. Wan, and T.-J. Zhang, “Cosmological constraints from radial baryon acoustic oscillation measurements and observational Hubble data,” *Physics Letters B*, **689**, 8–13 (2010), arXiv:1004.2599 [astro-ph.CO].
- [64] L. Verde, “Statistical methods in cosmology,” in *Lecture on Cosmology*, Lecture Notes in Physics, Vol. 800, edited by G. Wolschin (Springer, Berlin, 2010) pp. 147–177, ISBN 978-3-642-10597-5, arXiv:0911.3105 [astro-ph.CO].
- [65] A. G. Riess, L.-G. Strolger, J. Tonry, S. Casertano, H. C. Ferguson, B. Mobasher, P. Challis, A. V. Filippenko, S. Jha, W. Li, R. Chornock, R. P. Kirshner, B. Leibundgut, M. Dickinson, M. Livio, M. Giavalisco, C. C. Steidel, T. Benítez, and Z. Tsvetanov, “Type Ia supernova discoveries at $z > 1$ from the Hubble Space Telescope: Evidence for past deceleration and constraints on dark energy evolution,” *ApJ*, **607**, 665–687 (2004), arXiv:astro-ph/0402512.
- [66] C. Ma and T.-J. Zhang, “Power of observational Hubble parameter data: a figure of merit exploration,” preprint (2010), arXiv:1007.3787 [astro-ph.CO].
- [67] <http://www.physics.princeton.edu/act/index.html>.
- [68] N. Benítez, E. Gaztañaga, R. Miquel, F. Castander, M. Moles, M. Crocce, A. Fernández-Soto, P. Fosalba, F. Ballesteros, J. Campa, L. Cardiel-Sas, J. Castilla, D. Cristóbal-Hornillos, M. Delfino, E. Fernández, C. Fernández-Sopuerta, J. García-Bellido, J. A. Lobo, V. J. Martínez, A. Ortiz, A. Pacheco, S. Paredes, M. J. Pons-Bordería, E. Sánchez, S. F. Sánchez, J. Varela, and J. F. de Vicente, “Measuring baryon acoustic oscillations along the line of sight with photometric redshifts: The PAU survey,” *ApJ*, **691**, 241–260 (2009), arXiv:0807.0535.
- [69] P. Arnalte-Mur, A. Fernández-Soto, V. J. Martínez, E. Saar, P. Heinämäki, and I. Suhhonenko, “Recovering the real-space correlation function from photometric redshift surveys,” *MNRAS*, **394**, 1631–1639 (2009), arXiv:0812.4226.
- [70] D. Roig, L. Verde, J. Miralda-Escudé, R. Jimenez, and C. Peña-Garay, “Photo- z optimization for measurements of the BAO radial scale,” *Journal of Cosmology and Astro-Particle Physics*, **4**, 8 (2009), arXiv:0812.3414.
- [71] <http://www.sdss3.org/>.
- [72] P. McDonald and D. J. Eisenstein, “Dark energy and curvature from a future baryonic acoustic oscillation survey using the Lyman- α forest,” *Phys. Rev. D*, **76**, 063009 (2007), arXiv:astro-ph/0607122.

- [73] M. L. Norman, P. Paschos, and R. Harkness, “Baryon acoustic oscillations in the Lyman alpha forest,” *Journal of Physics Conference Series*, **180**, 012021 (2009), arXiv:0908.0964 [astro-ph.CO].
- [74] M. White, A. Pope, J. Carlson, K. Heitmann, S. Habib, P. Fasel, D. Daniel, and Z. Lukic, “Particle mesh simulations of the Ly α forest and the signature of baryon acoustic oscillations in the intergalactic medium,” *ApJ*, **713**, 383–393 (2010), arXiv:0911.5341 [astro-ph.CO].
- [75] Y. Wang, W. Percival, A. Cimatti, P. Mukherjee, L. Guzzo, C. M. Baugh, C. Carbone, P. Franzetti, B. Garilli, J. E. Geach, C. G. Lacey, E. Majerotto, A. Orsi, P. Rosati, L. Samushia, and G. Zamorani, “Designing a space-based galaxy redshift survey to probe dark energy,” *MNRAS*, in press (2010), arXiv:1006.3517 [astro-ph.CO].
- [76] R. Barkana and A. Loeb, “Probing the epoch of early baryonic infall through 21-cm fluctuations,” *MNRAS*, **363**, L36–L40 (2005), arXiv:astro-ph/0502083.
- [77] X.-C. Mao and X.-P. Wu, “Signatures of the baryon acoustic oscillations on 21 cm emission background,” *ApJ*, **673**, L107–L110 (2008), arXiv:0709.3871.
- [78] H.-J. Seo, S. Dodelson, J. Marriner, D. McGinnis, A. Stebbins, C. Stoughton, and A. Vallinotto, “A ground-based 21cm baryon acoustic oscillation survey,” *ApJ*, in press (2009), arXiv:0910.5007 [astro-ph.CO].